A turn-on fluorescent ion-imprinted polymer for selective and reliable optosensing of lead in real water samples

William René, Véronique Lenoble, Manel Chioukh, Catherine Branger

A turn-on fluorescent ion-imprinted polymer for selective and reliable optosensing of lead in real water samples

William René [a,b], Véronique Lenoble [b,*], Manel Chioukh[b], Catherine Branger [a,*]

[a] Université de Toulon, MAPIEM Laboratory, France

[b] Université de Toulon, Aix Marseille Université, CNRS/INSU, IRD, MIO UM 110, Mediterranean Institute of Oceanography, La Garde, France

* Corresponding authors: lenoble@univ-tln.fr, branger@univ-tln.fr

ABSTRACT

A new fluorescent Pb(II) imprinted polymer (Pb(II)-IIP) was synthesised for the selective detection of this contaminant in natural water. To play the sensing role, a fluorescent probe specific to Pb(II), based on anthracene coupled to 5-amino-8-hydroxyquinoline and a styrene moiety, was used as a functional monomer. It was associated with ethylene glycol dimethacrylate as cross-linker (EGDMA) to prepare microbeads of IIP and NIP (corresponding non-imprinted polymer) via precipitation polymerisation in DMSO-2-methoxyethanol (1:1, v/v) mixture. Solid-state ^{13}C NMR spectroscopy was used to analyse the structure of the polymers and attest the integration of the fluorescent monomer in the polymer matrix. The morphology of the prepared materials was analysed by scanning electron microscopy and nitrogen adsorption/desorption. Results showed high mesoporous materials with important surface areas of 346 and 232 $m^2.g^{-1}$ for IIP and NIP, respectively. Polymers fluorescence properties revealed that the obtained IIP showed remarkably selective fluorescent on-off characteristics towards Pb(II) compared to NIP, emphasizing an imprinting effect. IIP fluorescent calibration curve exhibited a linear range from 7.1 to 60 $\mu g.L^{-1}$ in pure water with a low limit of detection of 2.1 $\mu g.L^{-1}$. The synthesized IIP was successfully applied to the determination of Pb(II) in tap water, mineral water and seawater samples.

Keywords: Ion imprinted polymer; Fluorescence; Sensor; Lead

1. Introduction

Heavy metals accumulate in the environment and living bodies and pose significant threats to human health and the environment [1,2]. Lead is one of the most toxic heavy metals, presenting a huge impact on the global balance and food chains [3,4]. If inhaled or ingested, it may cause brain damages, anaemia or mental deficiency [5,6]. The major sources of lead pollution are mainly due to human activities like mining, fuel combustion and industrial processes [7]. The World Health Organization (WHO) sets the maximum lead concentration in drinking water at 10 $\mu g.L^{-1}$ [8]. Therefore, the determination of this

element is highly required for environmental sustainability and human health protection. Some analytical techniques such as atomic adsorption spectrometry (AAS) [9], inductive coupled plasma spectrometry (ICP-MS) [10] or anodic stripping voltammetry [11] are routinely used for lead detection. But these techniques are unsuitable for on-site analyses, with complex and expensive operation costs. Consequently, the development of new materials to design sensors for quick, sensitive and selective detection for lead is highly needed.

Molecularly imprinted polymers (MIPs) are synthetic polymers designed to mimic natural biological receptors to selectively recognize a target molecule [12]. The imprinting technology has been further extended to the recognition of other templates such as ions or proteins [13–15]. Thanks to their selective binding properties, the potential of imprinted polymers to act as recognition phases in biosensors was early identified [16] and they are ~~now~~ currently studied for that purpose with continuous and increasing efforts to improve their performances [17]. In this aim, MIPs or IIPs (ion imprinted polymers) can be turned into smart materials by introducing inside the polymer network a sensing probe that will directly transform the target binding into a measurable signal. This was achieved by a few teams for the electrochemical detection of organic compounds thanks to the use of a redox probe incorporated in MIPs as a functional monomer [18–20]. In a similar way, the use of fluorescent monomers becomes widespread to design fluorescent sensors based on MIPs [21–23]. Important advantages can be found through this concept as it does not require any external competiting probes, as in traditional indirect methods, and as it can be applied to the sensing of even non-fluorescent analytes. Furthermore, thanks to the direct interaction between the target molecule and the fluorescent probe, the sensitivity of the detection is improved. Although this model has been extensively used for the design of fluorescent MIPs [23], it remains more confidential for the detection of metal ions thanks to IIPs, with less than ten published works up to now. Hg(II) is the most studied ion, through exaltation [24,25] or quenching [26,27] of the fluorescence signal. Fluorescent IIPs have also been prepared for the detection of other metal ions such as Al(III) [28], Cu(II) [29,30], Ag(I) [31], Cd(II) [32] and Zn(II) [32].

To the best of our knowledge, no fluorescent IIP, incorporating a fluorescent monomer as the sensing element, has been prepared up to now for the selective detection of lead ions. In this work, the choice was made to use a fluorescent probe with a “turn-on” mode, that is to say, presenting an enhancement of its fluorescent signal upon Pb(II) binding. Indeed, such a mode was demonstrated to increase the sensitivity because of a lower optical background and higher signal-to-noise ratio [23]. This off-on effect can be produced thanks to an intramolecular photoinduced electron transfer (PET) process [33]. Upon this process, the binding of Pb(II) ion is expected to inhibit the electron transfer from the chelating group of the fluoroionophore towards the fluorescent moiety. This will result in an enhancement of the fluorescent signal. Based on this PET mechanism, ANQ, a fluoroionophore bearing a 5-amino-8-hydroxyquinoline group as the chelating group for Pb(II) recognition and anthracene as the fluorescent dye was chosen because of its intrinsic affinity for Pb(II) [34]. ANQ was modified into two fluorescent monomers: in ANQ-ST, ANQ was functionalized by a styrene polymerizable group and in ANQ-MMA

by a methyl methacrylate one [35]. A novel fluorescent IIP specific to Pb(II) could be developed by precipitation copolymerization of ANQ-ST with ethylene glycol dimethacrylate (EGDMA) as a crosslinker. The binding and selectivity properties of the IIP were investigated by three-dimensional fluorescence through the realisation of fluorescence excitation-emission matrices (EEMs). Thanks to this kind of analysis, the most favourable ($\lambda_{ex}/\lambda_{em}$) couple was optimized for each measurement which led to an improved quality and sensitivity of the analysis. In order to highlight the potential use of this IIP for the detection in real conditions, its performances were investigated on natural water samples.

2. Materials and methods

2.1. Reagents

$AgNO_3$, $CaCO_3$, $ZnSO_4$ and $NaNO_3$ were purchased from Fisher Scientific (Analytical grade), $Al(NO_3)_3$, $CdSO_4$, $Co(NO_3)_2$ and $CuSO_4$ from Merck (pro analysis grade), $Pb(NO_3)_2$ and $Fe(NO_3)_3$ from Carlo Erba (Analytical grade). Ethylene glycol dimethacrylate (EGDMA) was purchased from Fischer Scientific (98 %, contains 90-110 ppm monomethyl ether hydroquinone as inhibitor), methyl methacrylate (MMA) from Merck (99 %, contains 30 ppm MEHQ as inhibitor) and azobisisobutyronitrile (AIBN) from Merck (98 %). AIBN was purified prior use by recrystallization from methanol.

Solvents were purchased from Fischer Scientific (reagent grade). Dry solvents were purchased as extra dry grade (Fischer Scientific).

2.2. Instruments

^{13}C CP-MAS NMR spectra were recorded using Bruker Avance 400 MHz Ultrashield spectrometer at 100 MHz with magic angle spinning (MAS) frequency $\omega r/2\pi$ = 10 kHz. Scanning Electron Microscopy (SEM) images were taken using Supra40 VP microscope. Surface areas and pore volumes were determined by nitrogen adsorption/desorption experiments on a volumetric adsorption analyser Quantachrome Nova2200e (Quantachrome Instruments USA), at liquid nitrogen temperature. Inductively coupled plasma mass spectrometry ICP-MS (NexION® Series 300) was used for metals concentration determination. The Excitation-Emission Matrices (EEMs) of fluorescence were measured on a HITACHI F4500 spectrofluorimeter. The excitation wavelength ranged from 320 to 460 nm, with a step of 10 nm and an excitation slit of 1 nm. The corresponding emission spectra were acquired from 350 to 550 nm with a scan speed of 2400 $nm.min^{-1}$ and a slit of 1 nm. The photomultiplicator tension was fixed at 950 V and the integration time set at 0.1 s. The extraction of the 5 nm stepped emission was obtained by FL-Solution software. All the EEM of fluorescence were cleaned from the diffusion signals:

Rayleigh by cutting the diffusion band (20 nm) and Raman from first and second order by applying Zepp procedure [36].

2.3. Copolymerization of ANQ-ST and ANQ-MMA with MMA

30 mg of either ANQ-ST (((10-((4-vinylbenzyloxy)methyl)anthracene-9-yl)methyleneamino) quinoline-8-ol) or ANQ-MMA ((10-(8-hydroxyquinolin-5-ylimino)methyl)anthracen-9-yl)methyl methacrylate) were solubilized in 30 mL of THF in a 100 mL flask. 20 equivalents of MMA (121 mg for ANQ-ST polymerization and 134 mg for ANQ-MMA) were added and the mixture was purged with gentle flow of argon for 15 min. 20 mg of AIBN were added to the polymerization mixture and the solution was purged again with argon for 5 min and refluxed under argon for 24 hours. After cooling, the mixture was poured dropwise into 100 mL of ethanol. The formed precipitate was analysed by ^{1}H NMR spectroscopy.

2.4. Synthesis of fluorescent Pb(II)-IIPs particles

IIP and NIP particles were prepared by precipitation polymerization. In order to obtain particles, a total monomer weight fraction (ANQ-ST + EGDMA) versus solvent of 10% was chosen. AIBN was introduced with a 2% weight fraction towards the monomers. For IIP, ANQ-ST (0.46 mmol) was dissolved in 20 mL of DMSO-2-methoxyethanol (1:1, v/v) mixture in a 120 mL cylinder-shaped Pyrex tube. $Pb(NO_3)_2$ (0.23 mmol) was added and the solution was stirred for 30 min. Then EGDMA (8.40 mmol) was added and the solution was purged with a gentle flow of argon for 15 min. AIBN (0.25 mmol) was added to the polymerization mixture and the solution was purged again with argon for 5 min. The tube was introduced in a hybridation oven (HB-100 Hybridizer from UVP, UK) preheated at 30°C and rotated with a stirring rate of 8 rpm. The temperature was raised from 30 to 80°C with a ramp of 5°C every 15 min. The polymerization was stopped after 24 h. These parameters were intrinsic to the optimized precipitation polymerization. The resultant polymers were collected by filtration. They were sequentially washed four times with three different solvents: DMSO, dichloromethane and acetone, to remove the residual monomers. Then, to extract the template ion Pb(II), the polymer was placed in Corning® tubes and 20 mL of 0.1 $mol.L^{-1}$ EDTA solution were added. After 2 h of stirring and 2 h in an ultrasonic bath, the polymer was filtered. To assess the efficiency of the procedure, a control of the filtrate was performed by ICP-MS. Before the analyse, the filtrate was acidified with 20 µL of pure nitric acid. This washing step was repeated until Pb(II) concentration in the filtrate was close to the detection limit. Finally, the polymer was slightly ground (to disperse the particles) and dried under vacuum overnight. The microbeads of NIPs as a control polymer were prepared under identical conditions except for the omission of the template Pb(II).

2.5. Fluorescence measurements

The selectivity and binding properties of the IIP and the NIP were studied by three-dimensional fluorescence measurements. For all analysis, 3 mg of polymer were suspended in 3 mL of solvent in a quartz cuvette and the fluorescence was measured after 24h of stirring.

The fluorescence of the monomer ANQ-ST in a water-acetone (1:4, v/v) mixture was also measured in the presence of these different ions. Water-acetone mixture was optimised for the monomer fluorescence, as this molecule was not soluble in water [35]. Solutions containing 50 µmol.L^{-1} of ANQ-ST and 200 µmol.L^{-1} of an ion species were prepared and analysed for their fluorescence signal.

To study the polymers selectivity, 241 nmol.L^{-1} of Ag(I), Na(I), Ca(II), Cd(II), Co(II), Cu(II), Pb(II), Zn(II) or Al(III) was added to the suspension of polymer in a water-acetone (1:4, v/v) mixture. The fluorescence of IIP (or NIP) in presence of Pb(II) and an interfering ion was studied in a water-acetone (1:4, v/v) mixture. 241 nmol.L^{-1} of Pb(II) and 1 or 2 equivalents of interfering ions (i.e. Ag(I), Na(I), Ca(II), Cd(II), Co(II), Cu(II), Zn(II) or Al(III)) were added. These ions were chosen because of their potential competition towards Pb(II) retention, due to their higher concentration in ecosystems (major ions), their increasing concentration (e.g. Ag) or their similar charge (divalent metallic ions).

The fluorescent signal as a function of increasing lead concentration was studied in pure water, in water-acetone (1:4, v/v) mixture, in buffered water (HEPES buffer) at pH = 7.0 and 8.1, as well as in seawater (sampled in Toulon harbour (France)) and tap water (sampled in Toulon (France)). The last two matrices were filtered (0.2 µm syringe filters, cellulose nitrate, Sartorius®) before use. Increasing amounts of Pb(II) were added in the cuvette and after 24 h of stirring, the fluorescence signal was measured. The operation was repeated to obtain the complete range ($[Pb^{2+}]$ = 0-100 µg.L^{-1}).

Validation of lead determination was finally performed in seawater (sampled in Toulon harbour), tap water (sampled in Toulon) and in a mineral water (Evian®). All tested water samples were filtered through 0.2 µm syringe filters (cellulose nitrate, Sartorius®) before use. 10 µg.L^{-1} of Pb(II) was added and after 24 h of stirring, the fluorescence signal was measured with 3 replicates.

3. Results and discussions

3.1. Synthesis of fluorescent Pb(II)-IIP

As ANQ-ST and ANQ-MMA were new monomers that had never been incorporated in IIP, it was important to check their ability to polymerize. However, the characterization of highly crosslinked IIP is more difficult than the characterization of linear copolymer due to their insolubility. For this reason, polymerization tests were carried out with each monomer and MMA in THF to prepare linear copolymers which can easily be ~~easily~~ characterized by liquid phase NMR spectroscopy. MMA was chosen because its chemical structure is close to that of EGDMA, the crosslinker used for the preparation of the IIP particles. After 24 hours of reaction, the signals of ^{1}H NMR spectra corresponding to the vinyl

protons of ANQ-ST located at 6.77, 5.82 and 5.31 ppm disappeared (Fig. S1), whereas in the case of ANQ-MMA, the signals corresponding to the vinyl protons located at 6.10 and 5.57 ppm, remained unmodified (Fig. S2). These results showed that only ANQ-ST copolymerized with MMA in conditions similar to the preparation of imprinted polymers. As a consequence, ANQ-ST was selected for the preparation of the fluorescent Pb(II)-IIP particles.

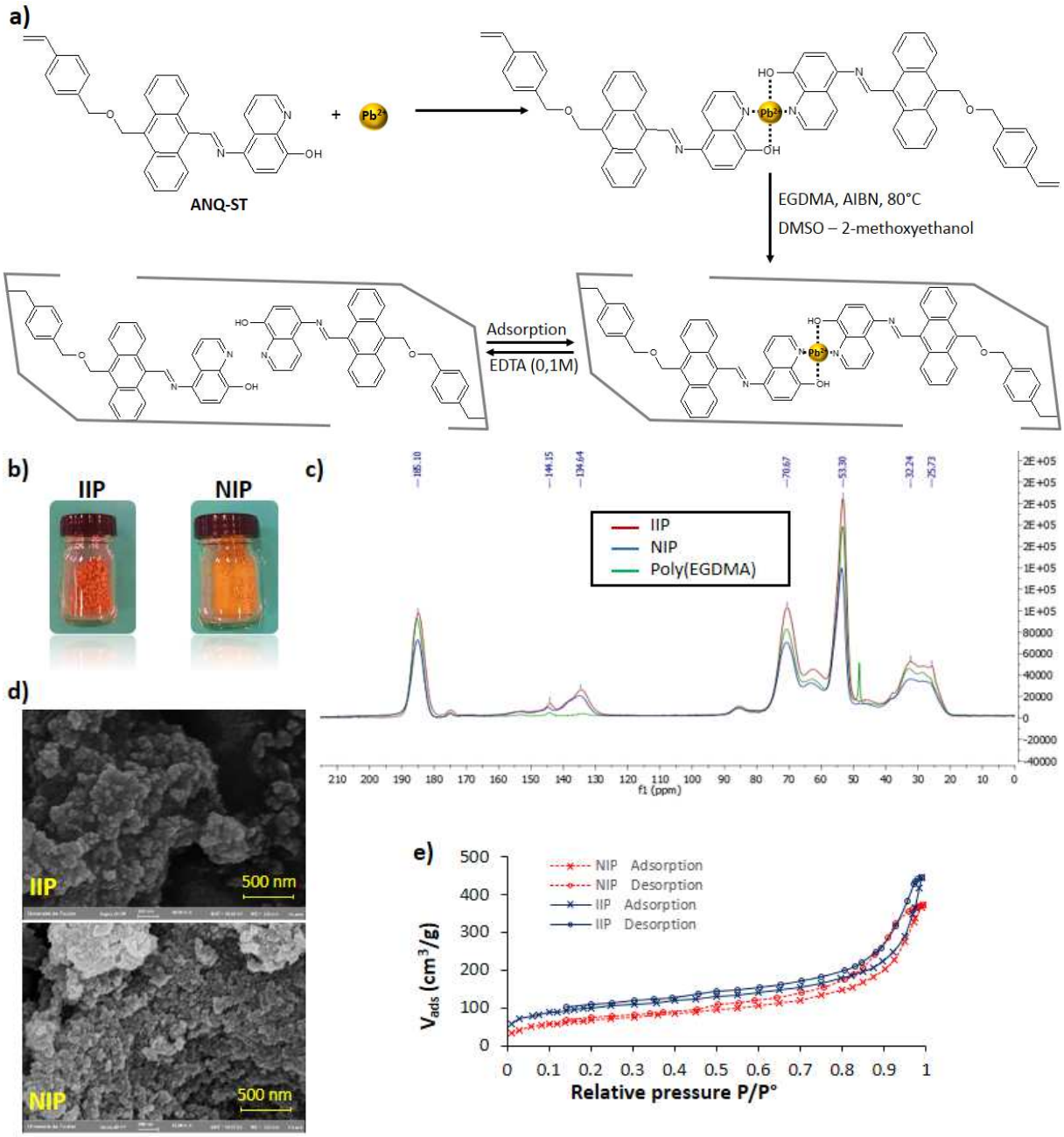

Fig. 1. *a) Synthesis route of Pb(II)-IIP, b) Pictures of the synthesized polymers, c) ^{13}C MAS NMR spectra of the polymers, d) Scanning electron microscopy pictures for IIP and NIP and e) Nitrogen adsorption/desorption isotherms of the prepared IIP and its corresponding NIP.*

The IIP and its corresponding non-imprinted polymer (NIP) were prepared by precipitation polymerization. This technique, widely used for the synthesis of imprinted polymers, offers the advantage to give micro or submicrosized particles [37] without the addition of any additive like surfactant [38]. It requires the wise choice of the polymerization solvent that will ensure both the solubilisation of the monomers in the initial stage of the polymerization and the precipitation of the polymer particles. Moreover, as far as imprinted polymers are concerned, the solvent must also act as a porogen agent. In the present case, highly polar DMSO was chosen to solubilise Pb(II) ions. However, attempts to copolymerize EGDMA and ANQ-ST in pure DMSO did not lead to the formation of particles, thus requiring the use of a co-solvent to ensure the precipitation of IIP. Further trials were carried out in DMSO-acetonitrile and DMSO-2-methoxyethanol mixtures (1:1, v/v). Only this last one was suitable to obtain IIP particles with a molar fraction of 5% of ANQ-ST. Although previous studies showed that higher amounts of functional monomer could optimize binding capacities [39], it was impossible to prepare IIP particles with higher rates of ANQ-ST fluorescent functional monomer. The synthesis scheme of the preparation of Pb(II)-IIP is shown in Fig. 1.a. Pb(II) ions and ANQ-ST were introduced with a 1:2 molar ratio to prepare the complex of stoichiometry 1:2. NIP was prepared according to the same procedure but without the presence of Pb(II). The IIP was obtained as a yellow-orange powder with a yield of 87 %. The NIP was obtained as a yellow powder with a yield of 98 % (Fig. 1.b). The colour difference could be attributed to the presence of Pb(II) template ions.

3.2. Chemical structure and morphology characterization of Pb(II)-IIP

The integration of the functional monomer ANQ-ST was assessed by the colour of the polymer since the yellow-orange colour is the tint of ANQ-ST and differs from the white colour of a poly(EGDMA). The integration was also confirmed by using the solid-phase ^{13}C CP-MAS NMR spectroscopy. Fig. 1.c shows ^{13}C CP-MAS spectra of poly(EGDMA), IIP and NIP. All these polymers presented signals of the poly(EGDMA) back-bone: the peak at 185.1 ppm assigned to the carbonyl of the ester function, the signal at 70.7 ppm to the carbons bound to the ether oxygen (-O-CH_2-CH_2-O-) and the peaks at 53.3, 32.7 and 26.3 ppm assigned respectively to quaternary, methylene and methyl carbons of the polymer chains. The integration of the functional monomer was evidenced by the peaks at 144.6 and 134.5 ppm, typical of aromatic carbons that were present only in ANQ-ST, not in EGDMA.

IIP and NIP morphologies were characterized by scanning electron microscopy (SEM) (Fig. 1.d). The synthesized IIP and the NIP consisted of aggregated nano-sized particles of 30-100 nm in diameter. This type of morphology is commonly observed in the literature for the synthesis of IIPs by precipitation polymerization [40–42]. From SEM observation, the polymers appeared to be very porous. Their textural properties were further investigated by nitrogen adsorption/desorption measurements, applying BET model for surface area determination and the BJH method for the evaluation of pore sizes and volumes. Polymers showed high surface areas of 346 and 232 $m^2.g^{-1}$ and pore volumes of 0.536 and

0.507 $cm^3.g^{-1}$ for IIP and NIP, respectively. According to the IUPAC classification, the obtained curves were type IV isotherms [43] (Fig. 1.e). This indicated that the polymers are mainly mesoporous, in accordance with the pore size diameters, measured at 6.0 and 8.3 nm. The highly porous structures of both IIP and NIP prove that the chosen polymerization solvent mixture correctly played the role of porogen, due to a high thermodynamical compatibility with the synthesized polymers [44].

.

3.3. Study of the Pb(II)-IIP selectivity

At first, the selectivity of the IIP and the NIP was evaluated in a water-acetone solution (1:4, v/v) in the presence of several ions, taken independently, such as Ag(I), Na(I), Ca(II), Cd(II), Co(II), Cu(II), Pb(II), Zn(II) or Al(III) (Fig. 2.a). Before Pb(II) addition, the EEMs showed a massive peak located at ($\lambda_{ex}/\lambda_{em}$) = 395/430 nm (with λ_{ex} = excitation wavelength and λ_{em} = emission wavelength) for IIP and at ($\lambda_{ex}/\lambda_{em}$) = 375/450 nm for NIP. Concerning IIP, it could be observed that only the addition of the template ion, Pb(II), induced a significant enhancement of the fluorescence signal. By comparison with the fluorescent probe, ANQ-ST which was as sensitive to Pb(II) as to Co(II), polymerisation therefore led to an improvement of the selectivity. Moreover, the signal increase caused by Pb(II) ions was more than twice more important in the case of IIP than for ANQ-ST. These observations proved that there was indeed an imprinting effect due to the chelation of Pb(II) by ANQ-ST during the synthesis of the imprinted polymer. This was in agreement with the study of the NIP behaviour. For this polymer, a fluorescent enhancement was also observed for Pb(II) but other ions like Zn(II) and Fe(III) had a more significant impact on the fluorescence signal. Besides, on the EEMs of NIP, it could be observed that the maximum of fluorescence intensity was sensitive to the tested ion, a variation which was not observed for IIP.

The sensing efficiency of the developed Pb(II)-IIP depends on its selectivity towards Pb(II) in the presence of competitive metal ions. Therefore, the fluorescence of the polymers was measured with Pb(II) and one or two equivalents of other interfering ion including Ag(I), Na(I), Ca(II), Cd(II), Co(II), Cu(II), Zn(II) and Al(III) (Fig. 2.c). Regarding the results, the impact of the addition of one equivalent of interfering ion was negligible on the IIP fluorescence in presence of Pb(II), which was not the case for NIP. The difference of binding behaviour of IIP compared to NIP was even more important in the presence of an excess (two equivalents) of interfering ion. For Cd(II), Zn(II) and Al(III), NIP fluorescence signal was strongly enhanced: up to 202% for Zn(II). These results emphasized the imprinting effect for IIP and its interesting properties to be used as a sensing element for Pb(II) detection.

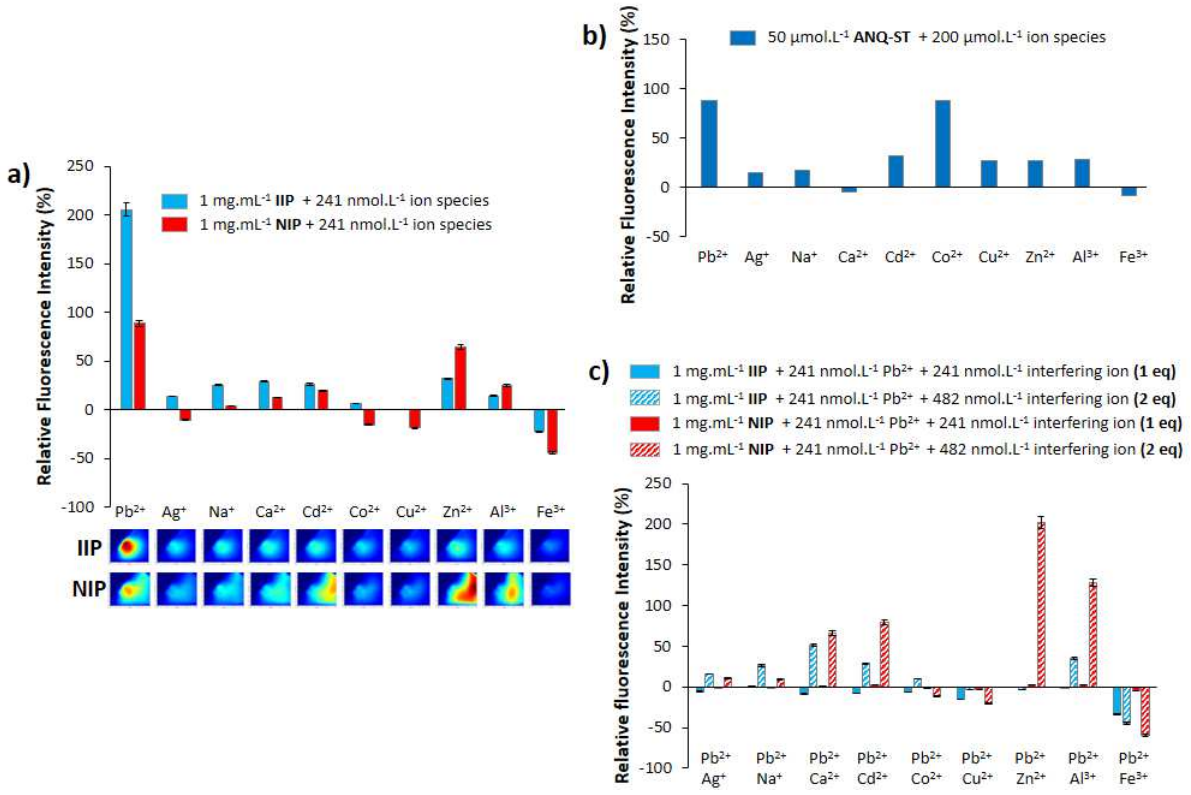

Fig. 2. *a) Relative fluorescence intensity (I-I_0)*100/I_0 of IIP/NIP in presence of various ion species and the corresponding fluorescence EEMs with I_0 the fluorescence intensity of IIP/NIP and I the fluorescence intensity of IIP/NIP in the presence of an ion species (241 nmol.L^{-1} of Pb(II) = 5 mg.L^{-1}), with ($\lambda_{ex}/\lambda_{em}$) = 395/430 nm for IIP and ($\lambda_{ex}/\lambda_{em}$) = 375/450 nm for NIP, b) Relative fluorescence intensity (I-I_0)*100/I_0 of the monomer ANQ-ST in the presence of various ions species with I_0 the fluorescence intensity of ANQ-ST and I the fluorescence intensity of ANQ-ST in the presence of an ion species, with ($\lambda_{ex}/\lambda_{em}$) = 400/430 nm and c) Relative fluorescence intensity (I-I_0)*100/I_0 of IIP and NIP in presence of Pb(II) and other interfering ions with I_0 the fluorescence intensity of IIP/NIP in the presence of Pb(II) alone and I the fluorescence intensity of IIP/NIP in the presence of Pb(II) and an interfering ion, with ($\lambda_{ex}/\lambda_{em}$) = 395/430 nm for IIP and ($\lambda_{ex}/\lambda_{em}$) = 375/450 nm for NIP.*

3.4. Study of Pb(II)-IIP binding capacities

To evaluate the fluorescent on-off properties and sensing capacities of the Pb(II)-IIP to Pb(II) ions, IIP and the NIP fluorescence were monitored in a water-acetone (1:4, v/v) mixture and in pure water at different concentrations of Pb(II). In water-acetone (1:4, v/v) mixture, the EEMs showed a massive peak located at ($\lambda_{ex}/\lambda_{em}$) = 395/430 nm for IIP and at ($\lambda_{ex}/\lambda_{em}$) = 375/450 nm for NIP. In pure water, the EEMs of fluorescence showed a massive peak located at ($\lambda_{ex}/\lambda_{em}$) = 395/430 nm for IIP and at ($\lambda_{ex}/\lambda_{em}$) = 370/450 nm for NIP. In both solvents, the relative peak intensities of the EEMs of IIP and NIP underwent a high enhancement upon Pb(II) binding. Fluorescence increase with increasing lead concentration came from the enhanced inhibition of electron transfer between the chelating group and the fluorescent moiety of the fluoroionophores corresponding to the PET process (as described in the Introduction). Fig. 3.a shows the fluorescence response of IIP and NIP at different concentrations of Pb(II) (from 0 to 100 µg.L^{-1}) in water-acetone (1:4, v/v) mixture and Fig. 3.b in pure water. The relative

fluorescence intensities were found to linearly increase up to 60 µg.L^{-1}, according to the equations (1) and (2) for IIP and NIP in water-acetone (1:4, v/v) mixture, and (3) and (4) in pure water:

$$\frac{I-I_0}{I_0} = 0.0398 * [Pb]\ (\mu g.L^{-1}) + 0.069 \quad (1)$$

$$\frac{I-I_0}{I_0} = 0.0197 * [Pb]\ (\mu g.L^{-1}) + 0.052 \quad (2)$$

$$\frac{I-I_0}{I_0} = 0.0279 * [Pb]\ (\mu g.L^{-1}) + 0.017 \quad (3)$$

$$\frac{I-I_0}{I_0} = 0.0095 * [Pb]\ (\mu g.L^{-1}) + 0.005 \quad (4)$$

High correlation coefficients of 0.9907 and 0.9424, in water-acetone mixture, were found for IIP and NIP, respectively, and 0.9719 and 0.9839 in pure water. In both solvents, the slope of the calibration line was higher for IIP than for NIP. The imprinting factor was evaluated as the ratio of the slopes of IIP upon that of NIP. Values of imprinting factor of 2.2 and 2.9 were determined in water-acetone (1:4, v/v) mixture and pure water respectively. These results proved that the imprinted polymer presents better properties for Pb(II) detection than NIP, with a higher imprinting effect in pure water.

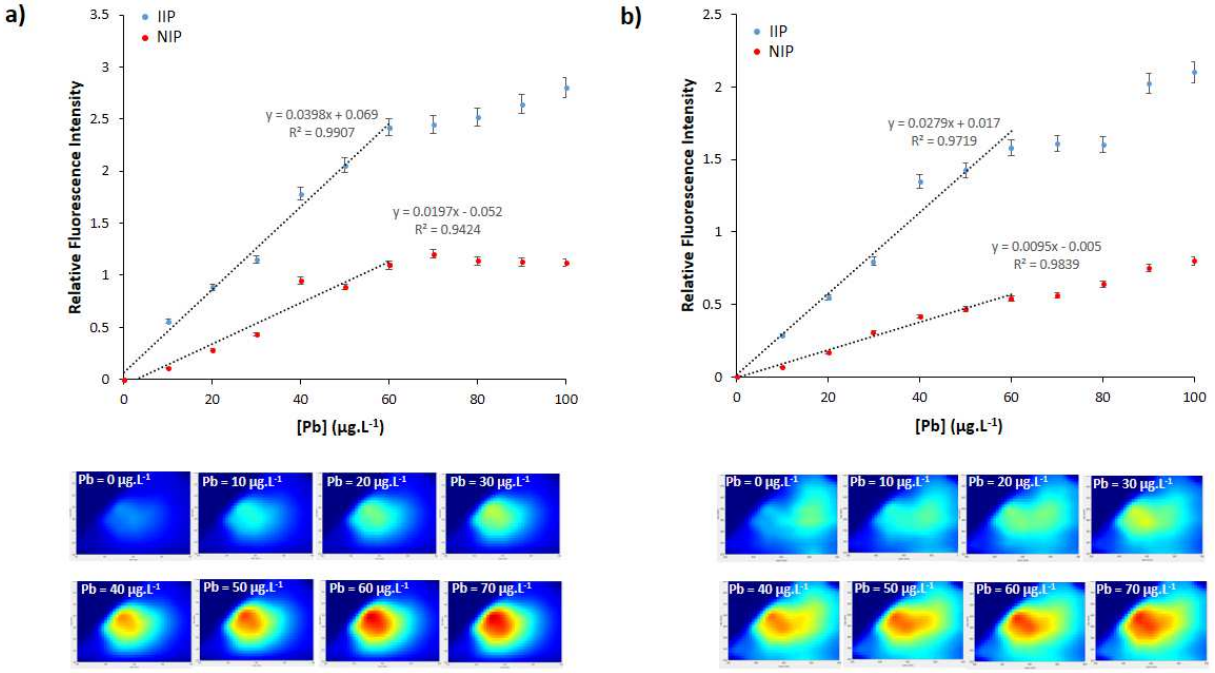

Fig. 3. *Calibration curves plotting the relative fluorescence intensity$(I-I_0)/I_0$ of IIP/NIP versus the concentration of Pb(II) and the corresponding fluorescence EEMs of IIP in a) a water-acetone (1:4, v/v) mixture with ($\lambda_{ex}/\lambda_{em}$) = 395/430 nm for IIP and ($\lambda_{ex}/\lambda_{em}$) = 375/450 nm for NIP and b) in pure water with ($\lambda_{ex}/\lambda_{em}$) = 395/430 nm for IIP and ($\lambda_{ex}/\lambda_{em}$) = 370/450 nm for NIP. With I the fluorescence intensity at a given concentration of Pb(II) and I_0 the intensity in the absence of Pb(II).*

With the aim of evaluating the analytical performance of the developed Pb(II) IIP, the limit of detection (LOD) was also investigated. Calculated as the concentration of Pb(II) that enhances three times the standard deviation of the blank signal as defined by IUPAC [45,46], the LOD was determined to be 2.1 µg.L^{-1} for IIP in pure water. This value is below the control level recommended by WHO for tap water (10 µg.L^{-1}). Up to now, only few papers report on ion determination via fluorescent IIPs and none

for Pb(II) detection. Table 1 focuses on works giving LOD and linear range data. Thus, compared to the literature, the Pb(II)-IIP designed in the present study appears to be the fluorescent IIP showing the best performances in terms of LOD and linear range of detection.

Table 1. *Fluorescent IIPs described in the literature and in the present work, and their main characteristics for metal detection*

Target Ion	***Effect of ion binding on the fluorescence***	***LOD*** *(nmol.L^{-1})*	***Linear range*** *(µmol.L^{-1})*	***Ref.***
Cu(II)	Quenching	40	0.16-8.29	[29]
Cu(II)	Quenching	140	0-70	[30]
Hg(II)	Quenching	20	0.05-1.2	[27]
Ag(I)	Exaltation	/	10-60	[31]
Hg(II)	Exaltation	150	0.28	[25]
Pb(II)	Exaltation	10	0.034-0.29	This work

In order to determine the effect of pH and of different matrices on the fluorescence signal, IIP spectra were carried out for Pb(II) concentrations varying from 0 to 50 µg.L^{-1} in pure water (pH = 5.9), in buffered water at pH = 7.0 and at pH = 8.1, in seawater (pH = 7.9) and in tap water (pH = 7.6). As shown in Fig. 4, under the different studied conditions, the obtained calibration curves present very close slopes. This proved that both pH and matrices have only little impact on the signal of fluorescence and thus on the detection and quantification of Pb(II) by the designed sensor.

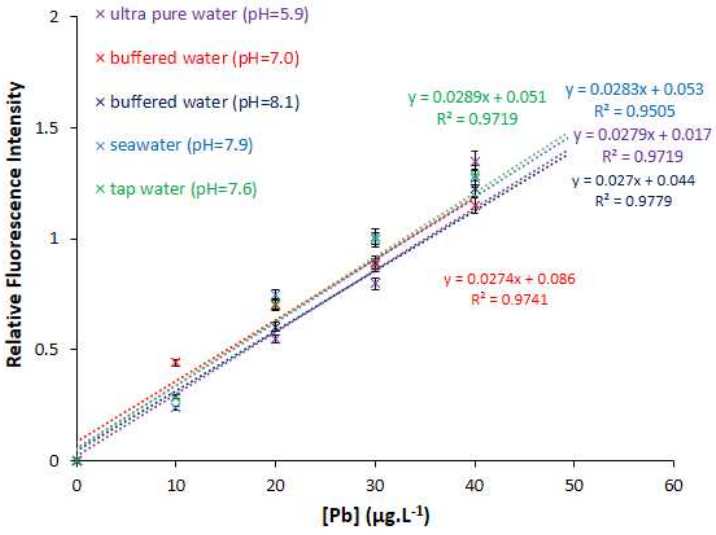

Fig. 4. *Plots of IIP relative fluorescence intensity versus the concentration of Pb(II) in different matrices with ($\lambda_{ex}/\lambda_{em}$) = 395/430 nm.*

3.5. Application to real sample analysis

In a final stage, the potential application of the developed fluorescent IIP as a IIP was validated by testing it on real water samples to selectively detect Pb(II). The samples were tap, mineral and seawater samples spiked with 10 µg.L^{-1} of Pb(II). The calibration curves previously established for tap water and seawater were used to quantify Pb(II) in these matrices by the fluorescent IIP. In the case of mineral

water, the calibration curve of buffered water (pH=7.0) was used. Excellent recovery rates in the range of 98-108 % were found (Table 2), demonstrating the real potential for IIP to be used as a sensor for direct Pb(II) detection in natural waters. It is noteworthy that even the high amounts of Ca(II) (80 $mg.L^{-1}$), Mg(II) (26 $mg.L^{-1}$) and Na(I) (6.5 $mg.L^{-1}$) ions present in the mineral water did not affect the measurements.

Table 2. *Determination of Pb(II) in real water samples spiked with lead.*

Sample	*Spike ($\mu g.L^{-1}$)*	*Found ($\mu g.L^{-1}$)*	*Recovery (%)*
Tap water (Toulon city, France)	10.0	9.8 ± 0.7	98
Mineral water (Evian®)	10.0	10.8 ± 2.2	108
Sea water (Toulon harbor, France)	10.0	10.3 ± 1.3	103

4. Conclusions

In the present paper, we aimed to design some new IIP including a fluorescent probe covalently attached to the polymer matrix for the detection of Pb(II). For this purpose, ANQ-ST was implemented as a new fluorescent probe functionalised by a styrene moiety. After optimisation of the solvent choice and the molar ratios of monomers, IIP particles were obtained by precipitation copolymerization of ANQ-ST with EGDMA as a crosslinker. The study of the selectivity properties of the IIP towards Ag(I), Na(I), Ca(II), Cd(II), Co(II), Cu(II), Pb(II), Zn(II) and Al(III) ions was achieved by three-dimensional fluorescence. It proved that, thanks to the imprinting effect, the selectivity was enhanced in the IIP compared to the initial molecular probe ANQ-ST and the NIP. The designed IIP presented a low limit of detection of 2.1 $\mu g.L^{-1}$ in pure water with a linear range of 7.1-60 $\mu g.L^{-1}$. Calibrations curves were established in various types of water: pure water, buffered waters (pH = 7.0 and 8.1), tap water and seawater. The very slight variations of slopes showed that the quantification of Pb(II) thanks to the IIP was not sensitive to matrix effects. The good recovery rates determined in these various samples proved that the designed fluorescent IIP is an efficient sensor for Pb(II) detection in environmental samples.

Acknowledgements

This work is part of the PREVENT program financed by the University of Toulon, Toulon-Provence-Méditerranée and the Conseil Départemental du Var, France. The authors acknowledge financial support from the Regional Council of Provence Alpes Côte d'Azur (France). They also want to thank Bruno Viguier for the ^{13}C NMR experiments.

References

[1] M.E. Mahmoud, M.M. Osman, Removal and preconcentration of lead (II), copper (II), chromium (II) and iron (III) from wate wastewaters by surface alumina adsorbents with immobilized 1-nitro-2-naphtol, J. Hazard. Mater. 173 (2010) 349–357.

[2] J. Gong, X. Wang, Adsorption of heavy metal ions by hierachically structured magnetite-carbonaceous spheres, Talanta. 101 (2012) 45–52.

[3] Z. Dahaghin, H.Z. Mousavi, S.M. Sajjadi, A novel magnetic ion imprinted polymer as a selective magnetic solid phase for separation of trace lead(II) ions from agricultural products, and optimization using a Box–Behnken design, Food Chem. 237 (2017) 275–281. https://doi.org/10.1016/j.foodchem.2017.05.118.

[4] T.J. Chow, Lead Accumulation in Roadside Soil and Grass, Nature. 225 (1970) 295.

[5] G. Gyananath, D.K. Balhal, Removal of lead (II) from aqueous solutions by adsorption onto chitosan beads, Cellul. Chem. Technol. 46 (2012) 121–124.

[6] G. Flora, D. Gupta, A. Tiwari, Toxicity of lead: a review with recent updates, Interdiscip. Toxicol. 5 (2012) 47–58.

[7] P. Sharma, R.S. Dubey, Lead toxicity in plants, Braz. J. Plant Physiol. 17 (2005) 35–52.

[8] S. Tong, von Schirnding, Praparmontol, Environmental lead exposure: a public health problem of global dimensions, Bull. World Health Organ. 78 (2000) 1068–1077.

[9] U. Divrikli, A.A. Kartal, M. Soylak, L. Elci, Preconcentration of Pb(II), Cr(III), Cu(II), Ni(II) and Cd(II) ions in environmental samples by membrane filtration prior to their flame atomic absorption spectrometric determinations, J. Hazard. Mater. 145 (2007) 459–464.

[10] G.A. Jenner, H.P. Longerich, S.E. Jackson, B.J. Fryer, ICP-MS — A powerful tool for high-precision trace-element analysis in Earth sciences: Evidence from analysis of selected U.S.G.S. reference samples, Chem. Geol. 83 (1990) 133–148.

[11] B.J. Feidman, J.D. Osterioh, Determination of lead in blood by square wave anodic stripping voltammetry at a carbon disc ultramicroelectrode, Anal. Chem. 66 (1994) 1983–1987.

[12] K. Mosbach, K. Haupt, Some new developments and challenges in non-covalent molecular imprinting technology, J. Mol. Recognit. 11 (1998) 62–68.

[13] J. Fu, L. Chen, J. Li, Z. Zhang, Current status and challenges of ion imprinting, J. Mater. Chem. A. 3 (2015) 13598–13627.

[14] G. Sharma, B. Kandasubramanian, Molecularly Imprinted Polymers for Selective Recognition and Extraction of Heavy Metal Ions and Toxic Dyes, J. Chem. Eng. Data. 65 (2020) 396–418.

[15] S. Ansari, S. Masoum, Molecularly imprinted polymers for capturing and sensing proteins: Current progress and future implications, TrAC Trends Anal. Chem. 114 (2019) 29–47.

[16] K. Haupt, K. Mosbach, Molecularly Imprinted Polymers and Their Use in Biomimetic Sensors, Chem. Rev. 100 (2000) 2495–2504.

[17] O.S. Ahmad, T.S. Bedwell, C. Esen, A. Garcia-Cruz, S.A. Piletsky, Molecularly Imprinted Polymers in Electrochemical and Optical Sensors, Trends Biotechnol. 37 (2019) 294–309.

[18] V. Mba Ekomo, C. Branger, R. Bikanga, A.-M. Florea, G. Istamboulie, C. Calas-Blanchard, T. Noguer, A. Sarbu, H. Brisset, Detection of Bisphenol A in aqueous medium by screen printed carbon electrodes incorporating electrochemical molecularly imprinted polymers, Biosens. Bioelectron. 112 (2018) 156–161.

[19] E. Mazzotta, A. Turco, I. Chianella, A. Guerreiro, S.A. Piletsky, C. Malitesta, Solid-phase synthesis of electroactive nanoparticles of molecularly imprinted polymers. A novel platform for indirect electrochemical sensing applications, Sens. Actuators B Chem. 229 (2016) 174–180.

[20] D. Udomsap, C. Branger, G. Culioli, P. Dollet, H. Brisset, A versatile electrochemical sensing receptor based on a molecularly imprinted polymer, Chem. Commun. 50 (2014) 7488–7491.

[21] O.Y.F. Henry, D.C. Cullen, S.A. Piletsky, Optical interrogation of molecularly imprinted polymers and development of MIP sensors: a review, Anal. Bioanal. Chem. 382 (2005) 947–956.

[22] S. Wagner, J. Bell, M. Biyikal, K. Gawlitza, K. Rurack, Integrating fluorescent molecularly imprinted polymer (MIP) sensor particles with a modular microfluidic platform for nanomolar small-molecule detection directly in aqueous samples, Biosens. Bioelectron. 99 (2018) 244–250.

[23] Q. Yang, J. Li, X. Wang, H. Peng, H. Xiong, L. Chen, Strategies of molecular imprinting-based fluorescence sensors for chemical and biological analysis, Biosens. Bioelectron. 112 (2018) 54–71.
[24] S. Lee, B.A. Rao, Y.-A. Son, A highly selective fluorescent chemosensor for Hg2+ based on a squaraine–bis(rhodamine-B) derivative: Part II, Sens. Actuators B Chem. 210 (2015) 519–532.
[25] T.H. Nguyen, A turn-on fluorescence-based fibre optic sensor for the detection of mercury, Sensors. 19 (2019) 2142.
[26] O. Güney, F.Ç. Cebeci, Molecularly imprinted fluorescent polymers as chemosensors for the detection of mercury ions in aqueous media, J. Appl. Polym. Sci. 117 (2010) 2373–2379.
[27] P.E. Hande, A.B. Samui, P.S. Kulkarni, Selective nanomolar detection of mercury using coumarin based fluorescent Hg(II)—Ion imprinted polymer, Sens. Actuators B Chem. 246 (2017) 597–605.
[28] S. Al-Kindy, R. Badía, M.E. Díaz-García, Fluorimetric Monitoring of Molecular Imprinted Polymer Recognition Events for Aluminium, Anal. Lett. 35 (2002) 1763–1774.
[29] S.C. Lopes Pinheiro, A.B. Descalzo, I.M. Raimundo, G. Orellana, M.C. Moreno-Bondi, Fluorescent ion-imprinted polymers for selective Cu(II) optosensing, Anal. Bioanal. Chem. 402 (2012) 3253–3260.
[30] Z. Xu, P. Deng, J. Li, S. Tang, Fluorescent ion-imprinted sensor for selective and sensitive detection of copper (II) ions, Sens. Actuators B Chem. 255 (2018) 2095–2104.
[31] H. Sun, J.-P. Lai, D.-S. Lin, X.-X. Huang, Y. Zuo, Y.-L. Li, A novel fluorescent multi-functional monomer for preparation of silver ion-imprinted fluorescent on–off chemosensor, Sens. Actuators B Chem. 224 (2016) 485–491.
[32] J. Tan, H.-F. Wang, X.-P. Yan, A fluorescent sensor array based on ion imprinted mesoporous silica, Biosens. Bioelectron. 24 (2009) 3316–3321.
[33] B. Valeur, I. Leray, Design principles of fluorescent molecular sensors for cation recognition, Coord. Chem. Rev. 205 (2000) 3–40.
[34] T. Anand, G. Sivaraman, A. Mahesh, D. Chellappa, Aminoquinoline based highly sensitive fluorescent sensor for lead(II) and aluminum(III) and its application in live cell imaging, Anal. Chim. Acta. 853 (2015) 596–601.
[35] W. René, M. Arab, K. Laatikainen, S. Mounier, C. Branger, V. Lenoble, Identifying the Stoichiometry of Metal/Ligand Complex by Coupling Spectroscopy and Modelling: a Comprehensive Study on Two Fluorescent Molecules Specific to Lead, J. Fluoresc. 29 (2019) 933–943.
[36] R.G. Zepp, W.M. Sheldon, M.A. Moran, Dissolved organic fluorophores in southeastern US coastal waters: correction method for eliminating Rayleigh and Raman scattering peaks in excitation–emission matrices, Mar. Chem. 89 (2004) 15–36.
[37] A. Beltran, F. Borrull, R.M. Marcé, P.A.G. Cormack, Molecularly-imprinted polymers: useful sorbents for selective extractions, TrAC Trends Anal. Chem. 29 (2010) 1363–1375.
[38] M.T. Gokmen, F.E. Du Prez, Porous polymer particles—A comprehensive guide to synthesis, characterization, functionalization and applications, Prog. Polym. Sci. 37 (2012) 365–405.
[39] W. Meouche, C. Branger, I. Beurroies, R. Denoyel, A. Margaillan, Inverse Suspension Polymerization as a New Tool for the Synthesis of Ion-Imprinted Polymers, Macromol. Rapid Commun. 33 (2012) 928–932.
[40] T. Alizadeh, S. Amjadi, Preparation of nano-sized Pb2+ imprinted polymer and its application as the chemical interface of an electrochemical sensor for toxic lead determination in different real samples, J. Hazard. Mater. 190 (2011) 451–459.
[41] V. Lenoble, W. Meouche, K. Laatikainen, C. Garnier, H. Brisset, A. Margaillan, C. Branger, Assessment and modelling of Ni(II) retention by an ion-imprinted polymer: Application in natural samples, J. Colloid Interface Sci. 448 (2015) 473–481.
[42] J. Otero-Romaní, A. Moreda-Piñeiro, P. Bermejo-Barrera, A. Martin-Esteban, Synthesis, characterization and evaluation of ionic-imprinted polymers for solid-phase extraction of nickel from seawater, Anal. Chim. Acta. 630 (2008) 1–9.
[43] K.S.W. Sing, Reporting physisorption data for gas/solid systems with special reference to the determination of surface area and porosity (Recommendations 1984), Pure Appl. Chem. 57 (1985) 603–619.
[44] O. Okay, Macroporous copolymer networks, Prog. Polym. Sci. 25 (2000) 711–779.

[45] G.L. Long, J.D. Winefordner, Limit of detection. A closer look at the IUPAC definition, Anal. Chem. 55 (1983) 712A–724A.
[46] V. Thomsen, D. Schatzlein, D. Mercuro, Limits of detection in spectroscopy, Spectroscopy. 18 (2003) 112–114.